MRS Advances © 2020 Materials Research Society
DOI: 10.1557/adv.2020.25

Facile Synthesis of Ceria Nanocrystals with Tuneable Size and Shape

Can Li[1], Yiliang Luan[1], Bo Zhao[2], Amar Kumbhar[3], Fan Zhang[4], Jiye Fang[1,4*]

[1]Department of Chemistry, State University of New York at Binghamton, New York, USA

[2]College of Arts & Sciences Microscopy, Texas Tech University, Texas, USA

[3]Chapel Hill Analytical and Nanofabrication Laboratory, University of North Carolina at Chapel Hill, North Carolina, USA

[4]Materials Science and Engineering Program, State University of New York at Binghamton, New York, USA

ABSTRACT

Ceria (CeO_2) possesses a distinctive redox property due to a reversible conversion to its nonstoichiometric oxide and has been considered as a promising catalyst in the oxidative coupling of methane. Since a heterogeneously catalytic process usually takes place only on the surface of catalysts, it is reasonably expected that the performance of a catalyst, such as CeO_2, highly relies on its size- and shape-dependent surface structure. We report our recent progress in achieving exclusive crystal facet-terminated CeO_2 nanocrystals using a shape-controlled synthesis protocol in a one-pot colloidal system. We modified a two-phase solvothermal approach to fabricate cubic and truncated octahedral CeO_2 nanocrystals with a size-control. During the two-phase solvothermal process, we propose that the Ce-precursors transfer from the aqueous layer to the interface of the organic phase, promoted by the capping ligands (as known as phase-transfer catalysts), for the oxidation and nucleation, and subsequently form CeO_2 nanocrystals in the organic layer. As different capping ligands favor binding on diverse crystal facets, tuning the composition of the capping ligand with a precise control could generate nanocrystals that are dominated by a single type of facets with a relatively narrow size distribution.

INTRODUCTION

As a most abundant rare earth element, cerium is now widely used in various fields, such as magnetics and catalysis[1-6]. Its oxide, ceria (CeO_2), is mainly utilized as a catalyst support or a catalyst directly. The typical examples include applications in three-way catalysts, fuel cell catalysts, solar cell media, and the methanol couple oxidation catalysts[6-11]. CeO_2, with a cubic crystal structure ($Fm\overline{3}m$, *225*), is also one of the most common catalysts for the oxidative coupling of methane. In order to enhance the size- and shape-dependent catalytic performance of CeO_2 nanocrystals, the development of an improved synthetic strategy with a surface character-control is potentially significant and has drawn growing attention recently[5, 12, 13].

In this study, we designed and fabricated size-controlled cubic, truncated octahedral and octahedral CeO_2 nanocrystals by adopting a robust two-phase solvothermal method with essential modifications. In these syntheses, the capping ligands (also known as phase-transfer catalysts) play a key role to control the size and morphology. We demonstrated that both the size and shape of the CeO_2 nanocrystals could be tuned by adjusting the functional group of a capping ligand. For instance, the presence of carboxyl groups (-COOH) within the stabilizing agents promoted the generation of {100}-facets to yield CeO_2 nanocubes, whereas the P=O derived functional group facilitates the formation of {111}-facets to produce CeO_2 nano-octahedra.

EXPERIMENT

Synthesis of CeO_2 nanocubes

The synthesis of {100}-dominated CeO_2 nanocubes was conducted using a method reported previously[12]. Typically, 7.5 mL of cerium nitrate ($Ce(NO_3)_3 \bullet 6H_2O$, Alfa Aesar, 99.5%) aqueous solution (16.7 mM) was added into a 20 mL Teflon-lined stainless-steel autoclave. 7.5 mL of toluene, 0.75 mL of oleic acid (OA, Sigma-Aldrich, 90%,) and 75 μL of *tert*-butylamine (TBA, TCI, >98%) were transferred into this autoclave, respectively. The sealed autoclave was then placed in a preheated oven at 180 ℃ and kept there for 24 h. After the autoclave was cooled to room temperature, the brownish and turbid upper organic layer was separated using a separatory funnel and collected. The products were then isolated by centrifugation after a sufficient amount of ethanol was added into the organic suspensions. The products (designed as "CeO_2 OA-nanocubes") were further purified by adding a mixture of hexane and ethanol (1:2 by vol.), ethanol (200 proof), and centrifugation in sequence for several cycles, and dried in a vacuum oven.

By replacing 0.75 mL of OA with 1216.0 mg of stearic acid (SA, TCI, >98%), uniform CeO_2 nanocubes could be fabricated. The rest of the recipe, synthetic procedure, and purification process were similar to those for CeO_2 OA-nanocubes. The final products are labeled as "CeO_2 SA-nanocubes".

Synthesis of CeO_2 nano-octahedra and truncated nano-octahedra

The {111}-terminated CeO_2 nano-octahedra were synthesized using a method reported previously[5,13]. Specifically, 2.5 mg of tri-potassium phosphate (K_3PO_4, Alfa Aesar, 97%) was dissolved in 15.0 mL of deionized water and 214.5 mg of $Ce(NO_3)_3 \bullet 6H_2O$ was dissolved in 2.5 mL of deionized water, respectively. Both solutions were mixed and transferred into a 50 mL Teflon-lined stainless-steel autoclave. The autoclave was then placed into a preheated oven at 180 ℃ and kept there for 12 h. The products (denoted as "CeO_2 nano-octahedra") were collected by adding a sufficient amount of ethanol into the resultant white and turbid suspensions, followed by centrifugation. The products were further purified by washing with a mixture of de-ionized water and ethanol (1:1 by vol.) and centrifugation in sequence for several cycles, dried in a vacuum oven.

To prepare CeO_2 truncated nano-octahedra, the synthetic recipe for CeO_2 OA-nanocubes was adopted while OA was replaced by trioctylphosphine oxide (TOPO, Sigma-Aldrich, 99%). In a typical synthesis, 7.5 mL of toluene, 75 μL of TBA and 835.0 mg of TOPO were added into a 20 mL Teflon-lined stainless-steel autoclave that contained 7.5 mL of $Ce(NO_3)_3$ solution (16.7 mM). The sealed autoclave was transferred to a preheated oven at 180 ℃ and kept there for 24 h. The generated brown and turbid upper layer was isolated using a separatory funnel and precipitated by adding a sufficient amount of ethanol, followed by centrifugation. The resultant products (acronymized as "CeO_2 truncated nano-octahedra") were re-dispersed in hexane and further washed using a mixture of oleic acid-hexane-ethanol (1:99:200 by vol.) for several cycles, and dried in a vacuum oven.

Characterization methods and preparation

X-ray diffraction (XRD) patterns were collected using a PANalytical X'pert X-ray powder diffractometer equipped with a Cu Kα1 radiation source. XRD samples were prepared by drop-casting concentrated nanocrystal suspensions of hexane onto a surface-polished Si holder for several times. An FEI Tecnai Spirit TEM operated at 120 kV was used for TEM imaging. To prepare the TEM samples, the CeO_2 nanocrystals were re-dispersed into hexane under an ultrasonication. One drop of as-prepared suspensions was drop-cast onto a Cu-based TEM grid (Tel Pella 01801) and dried naturally under ambient condition.

RESULTS AND DISCUSSION

Synthetic mechanism of CeO_2 nanocrystals

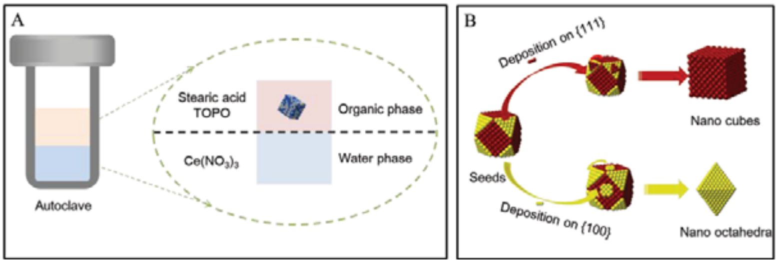

Figure 1. Illustration of the one-pot solvothermal synthesis process (A) and the shape-controlled synthetic mechanism of CeO_2 nanocrystals (B).

A two-phase solvothermal synthesis approach was utilized to synthesize CeO_2 OA-nanocubes, CeO_2 SA-nanocubes, and CeO_2 truncated nano-octahedra, as illustrated in Figure 1A. The top layer is an organic phase containing toluene as the organic solvent, whereas the bottom layer consists of water as the hydrophilic solvent. $Ce(NO_3)_3{\bullet}6H_2O$ was initially dissolved in the bottom layer to serve as the metal precursor. In this elevated-temperature process, it is believed that TBA can be hydrolyzed[12] gradually in the aqueous phase to generate an alkaline solution. It is also known that Ce(III) ions in such a basic environment could be converted to $Ce(OH)_3$[14, 15]. The generated $Ce(OH)_3$ can be further oxidized into $Ce(OH)_4$ by the dissolved O_2 from the air as indicated elsewhere[15-17]. Considering that in water the solubility of $Ce(OH)_4$ is much less than that of $Ce(OH)_3$ (K_{sp}^{o}: 2.0 x 10^{-48} *vs*. 1.6 x 10^{-20}) [18] and no CeO_2 product was harvested from the aqueous phase in this two-phase system, we would surmise that the oxidation would take place after the $Ce(OH)_3$ clusters migrate to the phase interface from the aqueous layer facilitated by the organic capping ligands[19, 20] (also known as phase transfer catalysts) and the hydrophobic CeO_2 nano-seeds should be generated and further evolved in the organic phase. Although the literature indicates that CeO_2 might be directly yielded[21] from the oxidation of Ce^{3+} under a high-pH condition in a single-phase aqueous solution as indicated in equation (1),

$$4\,Ce^{3+} + O_2 + 12\,OH^- \rightarrow 4\,CeO_2 + 6\,H_2O \quad (1)$$

we propose that even if Ce^{3+} ions were directly oxidized into CeO_2 in the two-phase system, it should likewise proceed on the interface between the aqueous and organic layers by taking the same facts into account. In the case of CeO_2 nano-octahedra, K_3PO_4 creates an alkaline environment for the oxidation of Ce^{3+}.

As shown in Figure 1B, the CeO_2 clusters/seeds, after migrating to the organic phase during the initial nucleation stage, would experience a subsequent growth in the presence of various functional capping ligands which have different binding affinities on a crystal facet. For example, OA or SA with a carboxyl functional group has a strong binding affinity to {100}-facets of CeO_2. These {100}-facets capped with OA or SA molecules reduce the growth rate along the direction of <001> and are stable, while other facets (such as {111} and {110}) are associated with relatively high growth rates along with their normal directions and rapidly eliminated during the crystal evolution stage. Thus, the functional capping ligands protect and preserve the {100}-facets, facilitating the formation of cubic nanocrystals. In the case of CeO_2 nano-octahedra, as another example, the PO_4^{3-} group promotes the binding on {111}-facets, resulting in octahedral nanocrystals.

Shape-controlled synthesis of CeO_2 nanocubes

OA was adopted as the phase-transfer catalyst and capping ligand for the synthesis of CeO_2 OA-nanocubes using a reported recipe[12]. The nanocubes were collected from the organic phase without further size-selection. Figure 2A presents a TEM image, showing that the as-prepared CeO_2 OA-nanocubes have a perfect cubic morphology but present a broad size distribution (20-200 nm in size). Additional results (not shown here) also indicate that the size of the nanocubes could be sensitively affected by other experimental factors such as the water/toluene ratio, the concentration of cerium precursor, and the amount of OA as well as TBA in the case of CeO_2 OA-nanocubes. Based on the observation in the product purification process, black and oily stuff was identified from the as-yielded products and it was difficult to be removed from the nanocrystals. This indicates that the C=C bonds from some OA molecules were possibly polymerized during the synthesis process, leading to a decrease of the OA fraction. It is believed that the large-size CeO_2 nanocubes could be formed through growth with an oriented aggregation of the crystal nuclei[12]. The insufficient OA as a capping ligand could cause such aggregation of the crystal nuclei, generating products in broader size distribution.

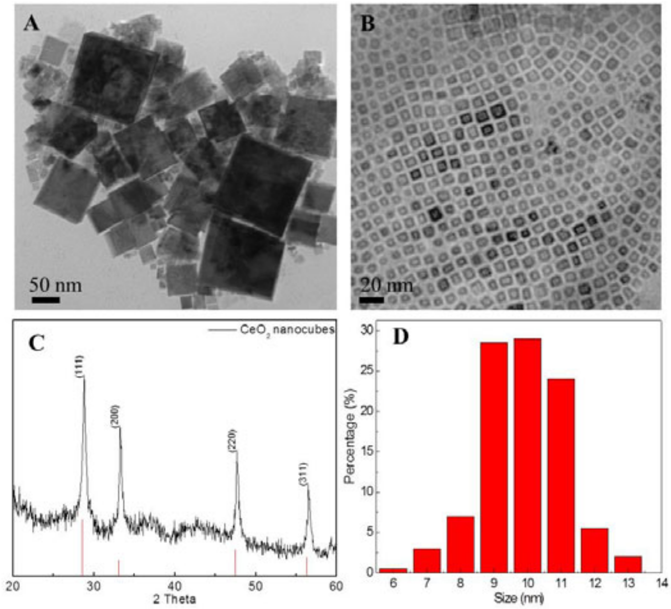

Figure 2. TEM images of CeO_2 OA-nanocubes (A), and CeO_2 SA-nanocubes (B), XRD pattern of the synthesized CeO_2 SA-nanocubes (C), and TEM-based size-distribution histogram of CeO_2 SA-nanocubes (D). The vertical lines on the bottom of (C) show standard XRD patterns of CeO_2 (ICDD PDF cards 34-0394).

To tackle this issue, OA was replaced by SA that contains the same carbon number and carboxyl group without the unsaturated bond. With SA, the size distribution of CeO_2 OA-nanocubes (average size: 10 nm) was indeed improved as shown in Figure 2B and 2D. The structure of CeO_2 SA-nanocubes was further examined using an XRD technique. Figure 2C presents a typical XRD pattern recorded from the CeO_2 SA-nanocubes. The four peaks in the XRD pattern are assigned to the diffraction planes of (111), (200), (220), and (311) from the ceria, respectively, which matches the standard CeO_2 XRD pattern very well (ICDD PDF cards 34-0394). It is worth pointing out that the intensity ratio between (200) and (111) peaks in Figure 2C is apparently higher than that from the standard XRD patterns (~0.68 *vs.* ~0.30). This is because some of the {100}-facets are perfectly aligned in this multi-layer XRD sample, leading to an enhancement of the (200) diffraction intensity.

Shape-controlled synthesis of CeO_2 nano-octahedra and truncated nano-octahedra

CeO_2 nano-octahedra were prepared using a conventional hydrothermal method[5,13] with a typical feature of large-scale production. The basic environment was originated from the hydrolysis of K_3PO_4, whereas PO_4^{3-} serves as a capping ligand to stabilize {111}-facet of CeO_2 nanocrystals. As shown in Figure 3A, the average size of CeO_2 nano-octahedra is ~200 nm. Even though the morphology and size-distribution are fairly uniform, the large size usually makes a catalyst difficult to be applied in an effectively catalytic process due to its low specific surface area.

To reduce the size, the two-phase solvothermal approach was applied to the CeO_2 octahedral synthesis. As PO_4^{3-} ligand played a key role in the aforementioned preparation, a replacement of PO_4^{3-} with organic phosphine or phosphate may act with a similar function in the organic phase. Trioctylphosphine, trioctylphosphate, and TOPO were investigated as the potential capping ligands to validate the shape-control effect. It was identified that TOPO is the best one to leverage the size- and shape-control of CeO_2 octahedra. As shown in Figure 3B, most of the CeO_2 nanocrystals exhibit a truncated-octahedral morphology with a size-distribution of 20 ± 2 nm. The CeO_2 truncated nano-octahedra are composed of both {100} and {111} facets, indicating that TOPO is able to stabilize both {111} and {100} facets. The structure of the CeO_2 truncated nano-octahedra was further confirmed by XRD (Figure 3C). All of the detectable peaks were identified as diffractions from (111), (200), (220), and (311) planes of the cubic phase CeO_2, respectively.

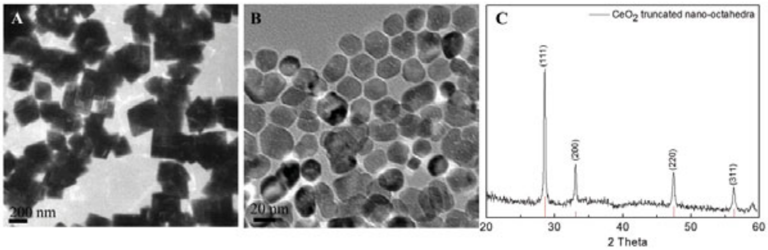

Figure 3. TEM images of CeO_2 nano-octahedra synthesized using K_3PO_4 (A), CeO_2 truncated nano-octahedra synthesized using TOPO (B), and XRD pattern of CeO_2 truncated-octahedra (C). The vertical lines on the bottom of (C) show standard XRD patterns of CeO_2 (ICDD PDF cards 34-0394).

CONCLUSIONS

In this work, CeO_2 nanocubes, truncated nano-octahedra, and nano-octahedra were synthesized using two-phase solvothermal and conventional hydrothermal approaches. We have demonstrated that the capping ligands with different functional groups play diverse roles in nanocrystal growth-control and shape-evolution. We further propose that the Ce^{3+} oxidation process wouldn't take place in the bulk aqueous phase in the two-phase syntheses. The crystal facet-tailored CeO_2 nanocrystals are inspired by the investigation in the oxidative coupling of methane for improved selectivity and C2 yield.

ACKNOWLEDGMENTS

This work was primarily supported by ACS PRF (58196-ND10). The TEM characterization was partially supported by CCMR (Cornell University) and S3IP (State University of New York at Binghamton). C.L. and F.Z. were partially supported by the Center for Alkaline-Based Energy Solutions, an Energy Frontier Research Center program supported by the US Department of Energy, under Grant DE-SC0019445; Y.L. was supported by NSF (DMR-1808383). C.L. acknowledges Dr. In-Tae Bae and Mr. John L. Grazul for their TEM training and assistance.

REFERENCES

1. Z. Hu, X. Liu, D. Meng, Y. Guo, Y. Guo and G. Lu. *ACS Catal.* **6**, 2265-2279 (2016).
2. L. Torrente-Murciano, A. Gilbank, B. Puertolas, T. Garcia, B. Solsona and D. Chadwick. *Appl. Catal. B* **132-133**, 116-122 (2013).
3. A.K.P. Mann, Z. Wu, F.C. Calaza and S.H. Overbury. *ACS Catal.* **4**, 2437-2448 (2014).
4. B. Zohour, D. Noon and S. Senkan. *ChemCatChem.* **6**, 2815-2820 (2014).
5. Y. Chen, Y. Chen, C. Qiu, C. Chenin and Z. Wang. *Mater. Lett.* **141**, 31-34 (2015).
6. T. Montini, M. Melchionna, M. Monai and P. Fornasiero. *Chem. Rev.* **116**, 5987-6041 (2016).
7. Y. Sun, Y. Shen, J. Song, R. Ba, S. Huang, Y. Zhao, J. Zhang, Y. Sun and Y. Zhu. *J. Nanosci. Nanotechnol.* **16**, 4692-4700 (2016).
8. J. Dou, Y. Tang, L. Nie, C.M. Andolina, X. Zhang, S. House, Y. Li, J. Yang and F. Tao. *Catal. Today.* **311**, 48-55 (2018).
9. A. Trovarelli and J. Llorca. *ACS Catal.* **7**, 4716-4735 (2017).
10. C. Yang, X. Yu, S. Heißler, A. Nefedov, S. Colussi, J. Llorca, A. Trovarelli, Y. Wang and C. Wöll. *Angew. Chem. Int. Ed.* **56**, 375-379 (2017).
11. Q. Tan, C. Shu, J. Abbott, Q. Zhao, L. Liu, T. Qu, Y. Chen, H. Zhu, Y. Liu and G. Wu. *ACS Catal.* **9**, 6362-6371 (2019).
12. S. Yang and L. Gao. *J. Am. Chem. Soc.* **128**, 9330-9331 (2006).
13. M. Zhang, Y. Chen, C. Qiu, X. Fan, C. Chen and Z. Wang. *Physica E Low Dimens.Syst. Nanost.* **64**, 218-223 (2014).
14. G. Svehla: Qualitative Inorganic Analysis, 7th ed. (Longman, Singapore, 1996), pp. 306.
15. P. Abellan, T.H. Moser, I.T. Lucas, J.W. Grate, J.E. Evans and N.D. Browning. *RSC Adv.* **7**, 3831-3837 (2017).
16. B. Bouchaud, J. Balmain, G. Bonnet and F. Pedraza. *J. Rare Earths.* **30**, 559-562 (2012).
17. P. Yu, S.A. Hayes, T.J. O'Keefe, M.J. O'Keefe and J.O. Stoffer. *J. Electrochem. Soc.* **153**, C74-C79 (2006).
18. J.T. Dahle and Y. Aras. *Int. J. Environ. Res. Public Health.* **12**, 1253 (2015).
19. J. Zhang, S. Ohara, M. Umetsu, T. Naka, Y. Hatakeyama and T. Adschiri. *Adv. Mater.* **19**, 203 (2007).
20. M. Brust, M. Walker, D. Bethell, D.J. Schiffrin and R. Whyman. *Chem. Commun.*, 801-802 (1994).
21. Z. Ji, X. Wang, H. Zhang, S. Lin, H. Meng, B. Sun, S. George, T. Xia, A.E. Nel and J.I. Zink. *ACS Nano.* **6**, 5366 (2012).